Coexistence of Intramolecular Ligand-Mediated and Through Hydrogen-Bond Magnetic Interactions in a Chain of Dicopper(II) Units

ARTICLE *in* INORGANIC CHEMISTRY · JUNE 2011

Impact Factor: 4.76 · DOI: 10.1021/ic200480d · Source: PubMed

8 AUTHORS, INCLUDING:

José Sánchez Costa
Laboratoire de Chimie de Coordination.
73 PUBLICATIONS **1,491** CITATIONS
SEE PROFILE

Boris Le Guennic
Université de Rennes 1
137 PUBLICATIONS **2,368** CITATIONS
SEE PROFILE

Guillaume Chastanet
French National Centre for Scientific Research
71 PUBLICATIONS **2,298** CITATIONS
SEE PROFILE

Laura Gasque
Universidad Nacional Autónoma de México
55 PUBLICATIONS **475** CITATIONS
SEE PROFILE

Inorganic Chemistry

ARTICLE

pubs.acs.org/IC

Coexistence of Intramolecular Ligand-Mediated and Through Hydrogen-Bond Magnetic Interactions in a Chain of Dicopper(II) Units

José Sánchez Costa,[§] Nuno A. G. Bandeira,[‡] Boris Le Guennic,*[,‡] Vincent Robert,[‡,¶] Patrick Gamez,*[,§,#] Guillaume Chastanet,[⊥] Luis Ortiz-Frade,[∥] and Laura Gasque*[,†]

[†]Facultad de Química, Universidad Nacional Autónoma de México, México 04510, D.F. México

[‡]Laboratoire de Chimie, Ecole Normale Supérieure de Lyon, CNRS, 46 Allée d'Italie 69364, Lyon Cedex 07, France

[§]Departament de Química Inorgànica, Universitat de Barcelona, Martí i Franquès 1-11, 08028 Barcelona, Spain

[#]ICREA, Passeig Lluís Companys, 23, 08010 Barcelona, Spain

[∥]Centro de Investigación y Desarrollo Tecnológico en Electroquímica, Pedro Escobedo, Querétaro, 76703, México

[⊥]CNRS, Université de Bordeaux, ICMCB, 87 avenue du Dr. A. Schweitzer, Pessac, F-33608, France

[¶]Laboratoire de Chimie Quantique, Institut de Chimie UMR 7177, CNRS and Université de Strasbourg, 4 rue Blaise Pascal, 67070 Strasbourg, France

Supporting Information

ABSTRACT: The reaction of 2,8-dimethyl-5,11-bis(pyridin-2-ylmethyl)-1,4,5,6,7,10,11,12-octahydroimidazo[4,5-h]imidazo-[4,5-c][1,6]-diazecine (dimp) with copper(II) nitrate in water produces the compound $[Cu_2(dimp)(H_2O)_2(NO_3)_2](NO_3)_2$. The single-crystal X-ray structure shows the formation of hydrogen-bonded chains in the lattice that are formed by dicopper(II) units doubly connected by nitrate/water bridges. Within the one-dimensional chains, the Cu ions are separated by either intramolecular or intermolecular distances of 7.309(2) Å or 6.255(2) Å, respectively. The magnetic susceptibility data revealing weak antiferromagnetic exchange interactions between the copper(II) ions were interpreted by considering two possible models, namely, an isolated dinuclear and a 1-D chain picture. The latter leads to an alternation $J_1 = -11.6$ and $J_2 = -3.0$ cm^{-1} along the chain. In order to clarify the relative strengths of the exchange couplings through hydrogen bonds and via the bridging dimp ligand, solution EPR studies and quantum chemical calculations were carried out. EPR studies unambiguously conclude on the existence of an exchange interaction J_a mediated by the dinucleating dimp ligand, while the through-H coupling J_b is physically absent in solution. On the basis of dinuclear units extracted from the X-ray data, J_a was estimated around -5.0 cm^{-1} from DFT-based calculations (M06 functional), whereas J_b is negligible. In contrast, wave function configuration interaction calculations (DDCI) support a description where both inter- and intramolecular pathways coexist with a preeminent role of H bonds with $J_a = -2.8$ and $J_b = -10.4$ cm^{-1}. Not only are these values very consistent with the extracted set of parameters (J_1, $J_2 = -11.6, -3.0$ cm^{-1}) but the possibility to generate leading exchange coupling through weak bonds is evidenced by means of wave function-based calculations.

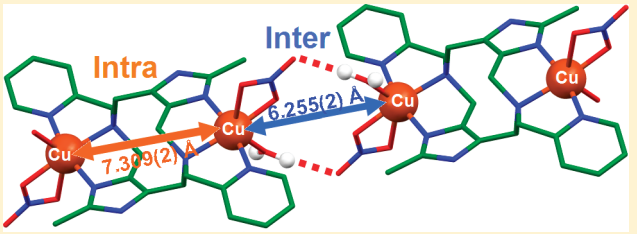

INTRODUCTION

The preparation of new ligands to control the organization of metal complexes at both the molecular and supramolecular levels is of great importance for the design of new polymetallic assemblies. Indeed, the interest shown by the scientific community for the preparation of polynuclear coordination compounds can be explained by the expectation of potential cooperativity between the metal ions. Indeed, such cooperativity might result in the modification of the electronic, magnetic, chemical, or catalytic properties that are not additive by comparison with two equivalents of the corresponding mononuclear analogues. For instance, numerous biological systems have nicely exploited this phenomenon for a large range of enzymatic processes, including the catalysis of nonredox hydrolysis;[1,2] reversible dioxygen binding and transport;[3−5] and the catalysis of multielectron redox reactions using valuable inorganic reactants such as O_2, N_2, H_2O, and H_2.[6−9]

Polymetallic complexes have always played a central role in molecular magnetic materials. Historically, the interest in molecular magnetism started in 1951 with the study of a simple dinuclear compound, namely, dicopper(II) tetra-acetate dihydrate.[10,11] Since then, numerous examples of dinuclear coordination compounds have been described, whose magnetic properties have been thoroughly investigated, shedding light on the mechanisms of exchange-coupling interactions.[12−16]

Received: March 8, 2011
Published: May 27, 2011

A possible approach to constructing dimetallic coordination compounds is to design and synthesize dinucleating ligands.[17−20] In addition, the ligands could possess several functions able to favor weak intermolecular interactions such as hydrogen bonds or $\pi-\pi$ stacking[21] and generate more complex architectures. With this goal in mind, some of us have developed recently a simple synthetic procedure, via a Mannich condensation, to prepare a new category of polydentate ligands based on a diazecine ring containing two imidazole groups.[22−27] In the present work, a copper(II) compound based on a member of this family of ligands, namely, 2,8-dimethyl-5,11-bis(pyridin-2-ylmethyl)-1,4,5,6,7,10,11,12-octahydroimidazo[4,5-h]imidazo-[4,5-c][1,6]-diazecine (dimp),[25] is reported. The resulting dicopper(II) compound $[Cu_2(dimp)(H_2O)_2(NO_3)_2](NO_3)_2$ was obtained from dimp and copper(II) nitrate. Let us mention that the catecholase activity of a perchlorate analogue has been highlighted recently.[28] The single-crystal X-ray structure of $[Cu_2(dimp)(H_2O)_2(NO_3)_2](NO_3)_2$ is described with special attention paid to the crystal packing since intermolecular contacts through hydrogen bonds may play a determinant role in the magnetic properties of the material. Indeed, magnetic interactions through H bonds in copper complexes have been already described experimentally[29−33] and addressed theoretically.[34,35] The magnetic properties of the present dinuclear Cu^{II} compound were analyzed on the basis of solid-state magnetic measurements and solution EPR spectroscopy. While the former have important implications for all of the possible exchange pathways, the latter cannot capture the challenging through-H mechanism we would like to examine in this particular compound. Therefore, quantum chemical calculations using either density functional theory (DFT) or multiconfigurational wave-function-based methods were used to identify the origin of the observed antiferromagnetic behavior, i.e., to quantify the respective contribution of hydrogen and covalent bonds. The use of DFT-based methods has proven to provide very satisfactory results for spin-coupled compounds. However, they may suffer from the arbitrariness of the exchange functional and the explicit treatment of weak-bond interactions. In order to complement this DFT-based analysis, complete active space self-consistent field (CASSCF) and subsequent difference dedicated configuration interaction (DDCI) and second-order perturbation (CASPT2) calculations were conducted. Dinuclear units consisting formally of two d^9 ions were extracted from the crystal structure. Following a bottom-up framework, the evaluation of the high-spin (triplet) and low-spin (singlet or broken-symmetry) energies gives access to the leading exchange coupling constants and eventually the relevant magnetic picture.

EXPERIMENTAL SECTION

Materials and Methods. 2-Picolylamine, 2-methylimidazole, and formaldehyde (37% aqueous solution) were purchased from Sigma-Aldrich and used without further purification.

Synthesis of 2,8-dimethyl-5,11-bis(pyridin-2-ylmethyl)-1,4,5,6,7,10,11,12-octahydroimidazo[4,5-*h*]imidazo[4,5-*c*]-[1,6]-diazecine (dimp). The ligand dimp was prepared according to the described procedure.[28] A total of 1.64 g (20 mmol) of 2-methylimidazole (**2**) was dissolved in 100 mL of distilled water together with 2.06 mL (20 mmol) of 2-picolylamine (**1**). To this mixture, 4.45 mL of formaldehyde (**3**) (37% aqueous solution; 60 mmol) was added dropwise with stirring. Finally, the pH was adjusted to 12 with concentrated KOH solution, and the solution was stirred at 60 °C for two days. The resulting precipitate was collected and washed with water. Anal. Calcd. for $C_{24}H_{28}N_8 \cdot 4H_2O$: C, 40.45; H, 4.49; N, 23.6. Found: C, 41.06; H, 4.75; N, 23.1.

Table 1. Crystal Data and Structure Refinement for $[Cu_2(dimp)(H_2O)_2(NO_3)_2](NO_3)_2$ (4)

empirical formula	$Cu_2C_{24}H_{32}N_{12}O_{14}$
F_w (g mol^{-1})	839.70
cryst syst	triclinic
space group	$P\bar{1}$
cryst color	blue
temperature (K)	298(2)
a (Å)	7.2780(19)
b (Å)	9.6850(15)
c (Å)	12.372(2)
α (deg)	96.140(13)
β (deg)	100.230(18)
γ (deg)	107.550(16)
V (Å^3)	806.2(3)
ρ_{calcd} (Mg/m^3)	1.730
μ (mm^{-1})	1.407
F(000)	430
θ for data collection (deg)	2.24−29.00
collected reflns	5081
independent reflns	4152
R_{int}	0.0649
R [$I > 2\sigma(I)$]	0.0743
wR (all data)	0.1913
goodness of fit on F^2	0.989
largest diff. peak and hole (e Å^3)	0.728 and −0.914

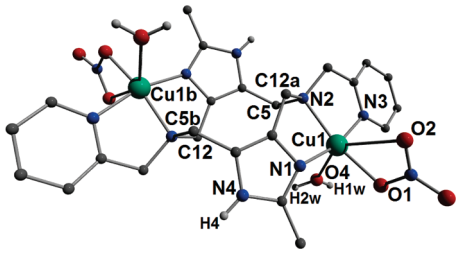

Figure 1. Representation of the molecular structure of the cation $[Cu_2(dimp)(H_2O)_2(NO_3)_2]^{2+}$ of compound **4**, illustrating the coordination environment of the copper(II) ion. Only the H atoms involved in hydrogen-bonding interactions are shown for clarity. Symmetry operation: $a = -x, 2 - y, -z$; $b = 1 - x, 2 - y, 1 - z$.

Synthesis of $[Cu_2(dimp)(H_2O)_2(NO_3)_2](NO_3)_2$ (4). This compound was obtained by gradually adding 0.5 mmol of solid dimp·$4H_2O$ to 1 mmol of $Cu(NO_3)_2 \cdot 2.5H_2O$ dissolved in 30 mL of water. Blue single crystals, suitable for X-ray diffraction, were collected after three days. Anal. Calcd. for $Cu_2C_{24}H_{32}N_{12}O_{14}$: C, 34.33; H, 3.81; N, 20.02. Found: C, 34.66, H, 4.02, N, 20.21.

X-Ray Crystallographic Analysis and Data Collection. Crystallographic data and refinement details are given in Table 1. The X-ray diffraction data were collected at 298(2) K with a Siemens P4/automatic diffractometer and analyzed using graphite-monochromated Mo Kα X-ray radiation (λ = 0.71073 Å). The structure was solved by Patterson methods using SHELXS 97-2.[36] Least-squares refinement based on F^2 was carried out by the full-matrix method of SHELXL 97-2.[36]

dx.doi.org/10.1021/ic200480d |*Inorg. Chem.* 2011, 50, 5696–5705

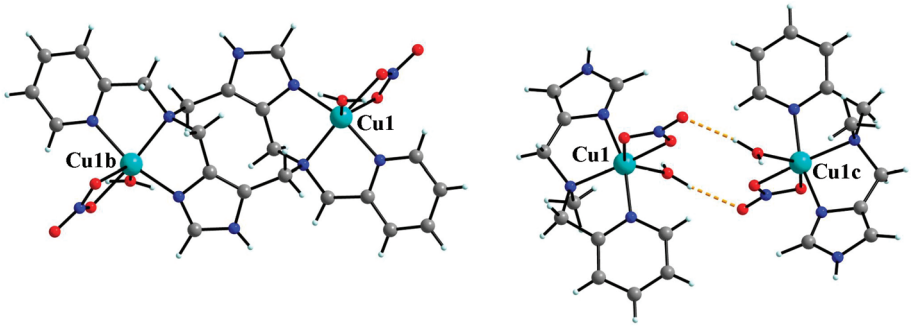

Figure 2. Dinuclear models **4a** (left) and **4b** (right) used in the DFT and CI calculations.

All non-hydrogen atoms were refined with anisotropic thermal parameters. In **4**, the anions present disorder with prolate displacement ellipsoids for the O atoms. The location of hydrogen atoms was generated geometrically and included in the refinement with an isotropic fixed thermal parameter using a "riding" model. Neutral atom scattering factors and anomalous dispersion corrections were taken from International Tables for Crystallography.[37] The molecular structure of the cationic part of compound **4** is shown in Figure 1.

Magnetic Measurements. The magnetic susceptibility data of powdered polycrystalline samples of **4** were recorded with a Quantum Design SQUID magnetometer. The molar magnetic susceptibility χ_M was investigated in the temperature range 2−325 K. The data were corrected for the experimentally determined contribution of the sample holder. Corrections for the diamagnetic response of the samples, due to closed atomic shells as estimated from the Pascal's constants,[38] were applied. The magnetic data were fitted using the Heisenberg spin Hamiltonian written as $H = -\Sigma_{(i,j)} J_{ij} S_i S_j$.

Computational Details. Calculations were performed on two distinct dinuclear units **4a** and **4b** (see Figure 2) ensuing from the crystallographic data, without any geometry optimization. To reduce the computational effort, the methyl groups were replaced by hydrogen atoms. First, density functional theory (DFT) calculations were carried out on both dinuclear models, with no symmetry constraints, using the ADF 2009.01 package.[39] Even if we are perfectly aware of the still ongoing discussion on which formulation is more valid for extracting J couplings from DFT energies,[40−44,71] we do not want to contribute further to the debate in this work. The exchange coupling parameter J was thus arbitrarily calculated on the basis of the broken symmetry (BS) method,[45,46] using the non spin-projected (NSP) expression

$$J = E(\mathrm{BS}) - E(\mathrm{T})$$

where E(BS) and E(T) are the total energies of the broken-symmetry and triplet states, respectively. Even if this expression is not the accepted as standard, it usually reproduces correctly the experimental values.[47−50] For the sake of completeness, let us state that for two magnetic centers with $s_z = 1/2$ such as Cu(II) ions, the spin-projected (SP) form gives J twice larger than the corresponding NSP values. Since the calculated energy difference is strongly dependent on the nature of the exchange-correlation functional,[51−54] we used both the pure GGA (generalized gradient approximation) BP86 functional[55,56] and the three-parameter hybrid functional of Becke based on the correlation functional of Lee, Yang, and Parr (B3LYP),[57,58] all employing the default local density functional based on the Vosko−Wilk−Nusair parametrization.[59] Finally, the hybrid meta-GGA M06 functional, developed by Truhlar and co-workers,[61] was used in our calculations since it has been shown recently that this functional provides excellent agreement between calculated and experimental exchange coupling constants of a series of dinuclear transition metal complexes.[54,62] All atoms were described with triple-ζ Slater-type basis sets with an additional polarization function (TZP).

To complement the DFT picture and clarify the magnetic role of the hydrogen bonds within the structures, complete active space self-consistent field (CASSCF)[63] calculations, including two electrons in two molecular orbitals (MOs), were performed by using the MOLCAS 7.2 package[64] to generate a reference space (CAS[2,2]), which consists of the configurations that qualitatively describe the problem. The local C_i symmetry of the adapted crystallographic model was taken into account in these multireference calculations to make them computationally tractable. The dynamical correlation effects were then incorporated on top of the triplet CASSCF wave function by using the dedicated difference configuration interaction (DDCI)[65,66] method implemented in the CASDI code.[67] With this approach, one concentrates on the differential effects rather than on the evaluation of the absolute energies. Such a strategy was successfully used to study the magnetic properties of various molecular and extended materials.[68−74] Nevertheless, this minimal active space picture may not be adapted to capture the hydrogen bond contributions to exchange coupling. As a matter of fact, it has been suggested that the whole H-bond network should be included. Some specific mechanisms involving the oxygen atom lone pairs and the bonding and antibonding OH group MOs are likely to stabilize the singlet over the triplet state. Thus, the minimal active space was enlarged to CAS[10,8] (10 electrons in 8 MOs) to evaluate the exchange coupling in **4b**.[35] Evidently, this strategy was not applied to **4a** since by construction this dinuclear unit does not contain hydrogen contacts. Since multireference second-order perturbation theory has shown already its ability to properly describe magnetic interactions,[75,76] CAS-[2,2]PT2[77,78] calculations were also carried out. All atoms were depicted with ANO-RCC type basis sets. The Cu atoms were described with a (21s15p10d6f4g2h)/[5s4p3d] contraction.[79] A (14s9p4d3f2g)/[3s2p1d] contraction was used for O and N, whereas a (14s9p4d3f2g)/[3s2p] contraction was used for C.[80] A (8s4p3d1f)/[2s1p] contraction was used for the H atoms involved in the hydrogen bonds, whereas a minimal basis set (8s4p3d1f)/[1s] was used for the other hydrogen atoms.[81]

EPR Measurements. EPR spectra of MeOH solutions at 77 K were recorded in the X band (9.85 GHz) using a Bruker ER200-SRC spectrometer with a cylindrical cavity.

RESULTS AND DISCUSSION

Synthesis. The ligand 2,8-dimethyl-5,11-bis(pyridin-2-ylmethyl)-1,4,5,6,7,10,11,12-octahydroimidazo[4,5-*h*]imidazo[4,5-*c*][1,6]-diazecine (dimp) (Scheme 1) was obtained following a synthetic procedure reported earlier for the preparation of related ligands.[23,25,26] Thus, the one-pot reaction of one equivalent of 2-picolylamine (**1**) with one equivalent of 2-methylimidazole (**2**) and two equivalents of formaldehyde (**3**; 37% aqueous solution) produces dimp with a yield of 25%. The reaction of two equivalents of copper(II) nitrate with one equivalent of ligand dimp in water under aerobic conditions produces blue crystals of

Scheme 1. Three-Component, One-Pot Synthesis of 2,8-Dimethyl-5,11-bis(pyridin-2-ylmethyl)-1,4,5,6,7,10,11,12-octahydroimidazo[4,5-*h*]imidazo[4,5-c][1,6]-diazecine (dimp)

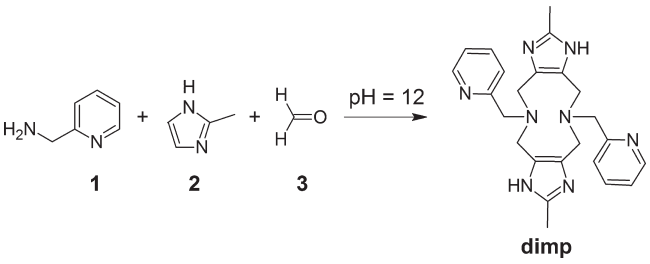

Table 2. Selected Bond Distances (Å) and Angles (deg) for $[Cu_2(dimp)(H_2O)_2(NO_3)_2](NO_3)_2$ (4)[a]

Cu1			
Cu1−N1	1.986(4)	O1−Cu1−N1	98.11(19)
Cu1−N2	2.079(5)	O1−Cu1−N3	94.90(18)
Cu1−N3	1.980(4)	N13−Cu1−N3	164.96(19)
Cu1−O1	2.011(4)	O1−Cu1−N2	165.65(18)
Cu1−O4	2.237(5)	N1−Cu1−N2	83.96(18)
Cu1−O2[b]	*2.606(5)*	N3−Cu1−N2	81.58(18)
		O1−Cu1−O4	84.76(19)
Cu1···Cu1b	7.309(2)	N1−Cu1−O4	94.45(19)
Cu1···Cu1c	6.255(2)	N3−Cu1−O4	94.21(19)
		N2−Cu1−O4	109.3(2)

[a] Symmetry operations: *b*, 1 − *x*, 2 − *y*, 1 − *z*; c, *x*, 1 + *y*, *z*. [b] Semicoordination bond.

4 after 3 days. The crystal structure as well as EPR spectroscopic studies in solution and solid-state magnetic data were obtained to characterize the magnetic properties of **4**. Theoretical investigations were then conducted to propose a magnetic description of the compound as accurately as possible.

Crystal Structure of $[Cu_2(dimp)(H_2O)_2(NO_3)_2](NO_3)_2$ (4). Single-crystal X-ray studies revealed that **4** crystallizes in the triclinic space group $P\bar{1}$. A view of the cationic part of **4** is represented in Figure 1. Details for the structure solution and refinement are summarized in Table 1, and selected bond distances and angles are listed in Table 2. The asymmetric unit of **4** contains one-half of the dinuclear complex molecule in general positions. An inversion symmetry operation generates the full molecule, giving a coordination compound of formula $[Cu_2(dimp)(H_2O)_2(NO_3)_2](NO_3)_2$ (**4**). The molecule is a dinuclear copper(II) compound consisting of five-coordinated metallic centers in a square-pyramidal environment (Figure 1). The base of the pyramid is formed by three N atoms belonging to a dimp ligand and one nitrate O atom, with the metal ion situated 0.1820(8) Å above the N1/N2/N3/O1 least-squares plane. The apical position is occupied by a water molecule. The coordination geometry around the copper(II) ions does not present unusual geometrical features, with Cu−N and Cu−O bond distances (Table 2) in normal ranges.[82,83]

The elongated Cu1−O4 distance (2.237(5) Å) compared to the Cu1−O1 one (2.011(4) Å) suggests the presence of an expected Jahn−Teller distortion.[84] The bond lengths Cu1−N1 (1.986(4) Å) and Cu1−N(3) (1.980(4) Å) are fairly equivalent

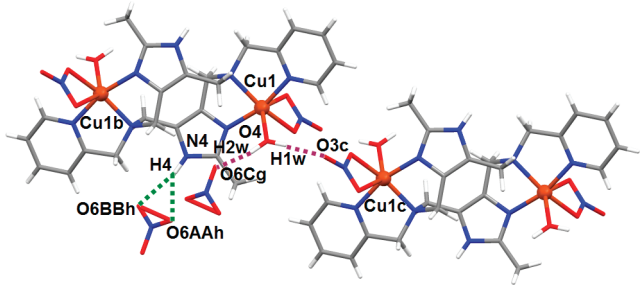

Figure 3. Illustration of the crystal lattice of **4** showing the hydrogen-bonding interactions. O4−H1w···O3c = 2.883(7) Å; O4−H2w···O6Cg = 2.724(7) Å; N4−H4···O6Aah = 2.939(13) Å; N4−H4···O6BBh = 3.11(2) Å. The Cu1··· Cu1b and Cu1··· Cu1c separation distances are 7.209(2) and 6.255(2) Å, respectively. Symmetry operations: c = *x*, 1 + *y*, *z*; g = −1 + *x*, *y*, *z*; h = 1 − *x*, 1 − *y*, −*z*.

Table 3. Hydrogen-Bonding Parameters for $[Cu_2(dimp)(H_2O)_2(NO_3)_2](NO_3)_2$ (4)[a]

D−H···A	H···A (Å)	D···A (Å)	∠(D−H···A) (deg)
O4−H1w···O3c	1.99	2.883(7)	172.7
O4−H2w···O6Cg	1.83	2.724(7)	168.1
N4−H4···O6AAh	2.18	2.939(13)	146.8
N4−H4···O6BBh	2.27	3.11(2)	168.0

[a] Symmetry operations: c = *x*, 1 + *y*, *z*; g = −1 + *x*, *y*, *z*; h = 1 − *x*, 1 − *y*, −*z*.

and shorter than the Cu1−N2 distance (2.079(5) Å). This feature can be attributed to the π-acceptor character of the aromatic nitrogen atoms N1 and N3. The geometric parameter τ amounts to 0.10, therefore indicating an almost perfect square-pyramidal geometry (τ = 0.00 for a square pyramid and 1.00 for a trigonal bipyramid[84]). In addition, the Cu1 ion is semicoordinated by the nitrate oxygen atom O2 (Cu1−O2 = 2.606(5) Å), illustrating a chelating character of the NO_3^- ion. The 10-membered central (1,6) diazecine ring adopts a chair conformation, with a total puckering amplitude of 1.919 Å.

In the crystal lattice, the dinuclear copper(II) molecules are involved in a hydrogen-bonding network (Figure 3 and Table 3). Thus, the imidazole hydrogen atom H4 is bonded to a disordered nitrate anion (N4−H4···O6AAh = 2.939(13) Å and N4−H4···O6BBh = 3.11(2) Å; Figure 3). Both hydrogen atoms of the coordinated water molecule are strongly interacting with H-bond acceptor atoms, namely, the oxygen atom O6Cg from a noncoordinated nitrate ion (O4−H2w···O6Cg = 2.724(7) Å) and the oxygen atom O3c from a coordinated nitrate ion (O4−H1w···O3c = 2.883(7) Å) belonging to a neighboring dicopper(II) unit (Figure 4). The latter hydrogen-bonding contacts, occurring along the crystallographic *c* axis, connect the dinuclear molecules through double $O_{water}-H\cdots O_{nitrate}$ bridges (red rectangle in Figure 4), to generate a one-dimensional (1-D) supramolecular chain. Within these 1D chains, the copper(II) ions are separated by an intramolecular distance of 7.309(2) Å (Cu1···Cu1b) and by an intermolecular distance of 6.255(2) Å (Cu1···Cu1c). The 1D chains are further associated with each other, via an intricate network of $\pi-\pi$[86] and anion$-\pi$[87] interactions (Figures 4 and Figure S1, Supporting Information). Hence, $\pi-\pi$ stacking interactions are observed between imidazole rings (Cg4···Cg4′ = 3.924(4) Å; Figure 4

dx.doi.org/10.1021/ic200480d |*Inorg. Chem.* 2011, 50, 5696–5705

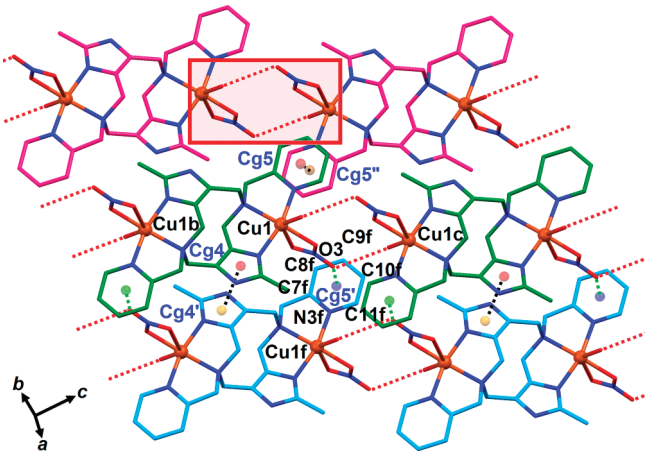

Figure 4. Representation of the crystal packing of **4** showing the $\pi-\pi$ and anion$-\pi$ interactions. Cg4$\cdots$Cg4′ = 3.924(4) Å; Cg5$\cdots$Cg5″ = 3.669(4) Å; O3$\cdots$Cg5′ = 3.059(7) Å. The red rectangle highlights the double $O_{water}-H\cdots O_{nitrate}$ bridges that generate a supramolecular 1D chain. The interchain Cu1$\cdots$Cu1f and Cu1c$\cdots$Cu1f separation distances are 7.278(2) and 7.852(2) Å, respectively. Symmetry operations: b = $1-x, 2-y, 1-z$; c = $x, 1+y, z$; f = $1+x, y, z$.

Table 4. Contact Distances (Å) and Angles (deg) Characterizing the $\pi-\pi$ Interactions and the O3$\cdots$Pyridine (Cg5′) Bonding Interaction in 4 and Interchain Cu$\cdots$Cu Separation Distances[a]

Cg4$\cdots$Cg4′	3.924(4)	Cg5$\cdots$Cg5″	3.669(4)
O3−N3f	3.278(8)	O3−C7f	3.363(9)
O3−C8f	3.445(9)	O3−C9f	3.441(9)
O3−C10f	3.335(10)	O3−C11f	3.245(9)
O3−Cg5′	3.059(7)		
O3−Cg5′−pyridine plane	85.36(18)		
Cu1$\cdots$Cu1f	7.278(2)	Cu1c$\cdots$Cu1f	7.852(2)

[a] Symmetry operations: b = $1-x, 2-y, 1-z$; c = $x, 1+y, z$; f = $1+x, y, z$.

and Table 4) and between coordinated pyridine moieties (Cg5$\cdots$Cg5″ = 3.669(4) Å; Figure 4 and Table 4). Moreover, the nitrate oxygen atom O3 is strongly interacting with a coordinated pyridine from an adjacent 1D chain, as confirmed by the O3$\cdots$pyridine centroid (Cg5′) distance of 3.059(7) Å (Table 4). Indeed, this contact distance is below the minimum distance, namely 3.08 Å, considered when defining a bonding interaction between a nitrate oxygen atom and a pyridine ring.[88] The contact distances O3−$C_{pyridine}$ (Table 4) are close to the corresponding sum of van der Waals radii,[88] and the O3−$N_{pyridine}$ separation distance is just above the corresponding sum of van der Waals radii.[89] The angle O3−Cg5′−pyridine plane of 85.36(18)°, close to the ideal value of 90°,[90] further confirms the strong bonding interaction between the nitrate O3 ion and the pyridine ring (N3f, C7f, C8f, C9f, C10f, C11f).

Magnetic Properties. The $\chi_M T$ and χ_M versus T plots for a polycrystalline sample of compound **4**, recorded under a constant magnetic field of 0.1 T in the temperature range 2−300 K, are shown in Figure 5 (χ_M being the molar magnetic susceptibility). The value of $\chi_M T$ at room temperature is higher than that expected for two uncoupled copper(II) centers (1.08 cm^3 K mol^{-1} instead of 0.75 cm^3 K mol^{-1} for g = 2.0).

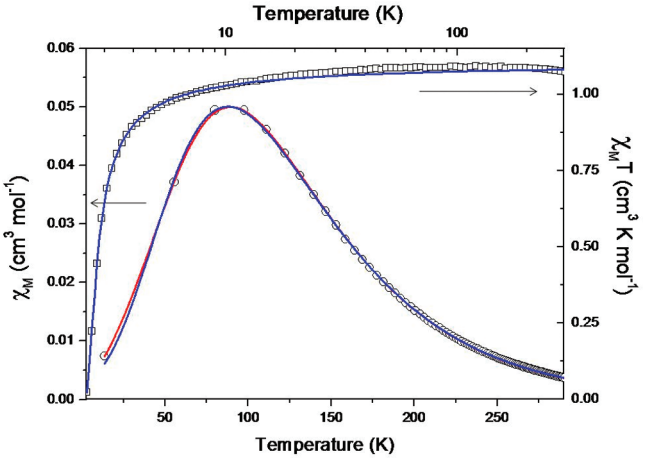

Figure 5. Variations of the molar magnetic susceptibility of **4** with the temperature, drawn as the $\chi_M T$ vs T (empty square, right and down scale) and χ_M vs log(T) (empty circles, left and upscale) curves. The blue and red solid lines are fits to the experimental data, as discussed in the text.

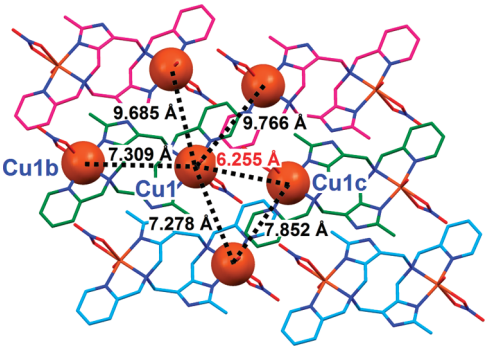

Figure 6. Different Cu$\cdots$Cu separation distances found in the solid-state structure of **4**. Symmetry operations: b = $1-x, 2-y, 1-z$; c = $x, 1+y, z$.

By decreasing the temperature, $\chi_M T$ remains constant until about 75 K, where it starts to decrease to reach a diamagnetic value at 2 K while χ_M exhibits a maximum at 9.5 K. This indicates the presence of antiferromagnetic interactions within the sample.

The crystal packing of **4**, which is driven by hydrogen-bonding, $\pi-\pi$ stacking, and anion$-\pi$ interactions (see above), reveals a number of intra- and intermolecular Cu$\cdots$Cu separation distances (see Tables 2 and 4 and Figure 6) varying from 6.255(2) to 9.766(2) Å. Regarding the intracopper contact Cu1$\cdots$Cu1b (7.309(2) Å), the presence of sp^3 carbons between the two binding pockets (carbon atoms C5, C5b, C12, and C12a in Figure 1) was first thought to disrupt a potential ligand-mediated exchange among the two Cu^{II} ions, the π-conjugation between the four aromatic donor rings being therefore interrupted. On the other hand, the Cu1−Cu1c dinuclear fragment formed by the two Cu−O_2NO$\cdots$HO(H)Cu paths (see model **4b** in Figure 2) is characterized by the shortest metal−metal separation distance (6.255(2) Å). Moreover, the magnetic exchange between copper(II) centers through hydrogen-bonding interactions involving coordinated water molecules is well-exemplified in the literature,[32] even if the participation of a coordinated

dx.doi.org/10.1021/ic200480d |*Inorg. Chem.* 2011, 50, 5696–5705

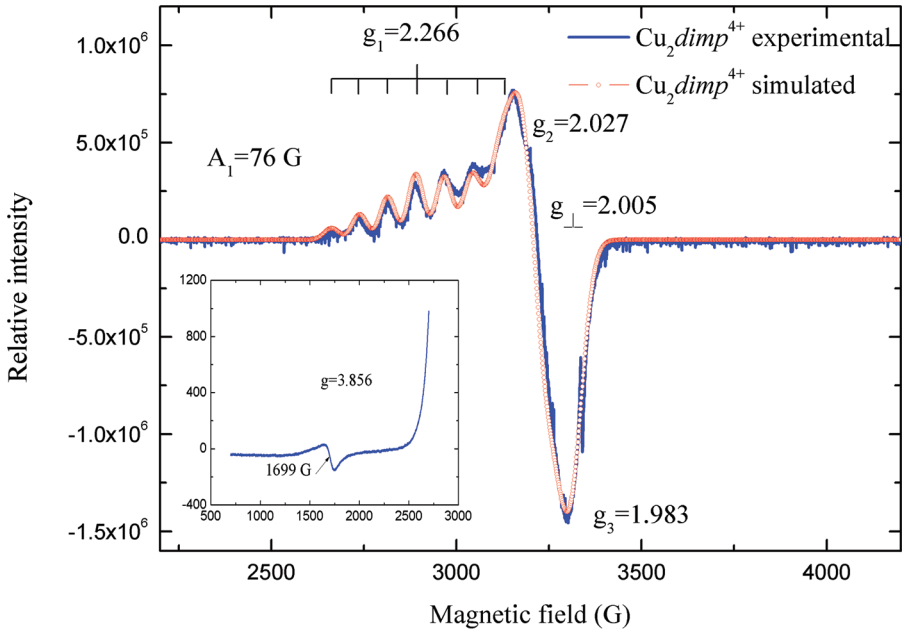

Figure 7. Simulated (red) and experimental (blue; frozen MeOH) EPR spectra for $[Cu_2(dimp)(H_2O)_2](NO_3)_4$. The inset shows the half-field signal.

nitrate anion in this magnetic-exchange pathway is rather unusual. Therefore, the magnetic behavior of compound **4** can be interpreted on the basis of two distinct models. The first one consists of a copper(II) dinuclear model according to the Bleaney–Bowers[10] equation (eq 1) and takes into account possible intermolecular interactions through the introduction of a zJ' term. A second model considers a hydrogen-bonded 1-D chain of dinuclear molecules. In this line, we used the alternating antiferromagnetic $S = 1/2$ chain model of Hatfield.[90]

$$\chi_M = 2Ng^2\beta^2\left[kT - \frac{2zJ'}{3 + e^{-J/kT}}\right]^{-1}[3 + e^{-J/kT}]^{-1} \qquad (1)$$

The least-squares fitting of the data (blue lines in Figure 5) applying eq 1 leads to $g = 2.42$, $J = -11.40$ cm^{-1}, and $zJ' = -2.32$ cm^{-1}. The small J value observed, comparable to those reported for similar compounds described in the literature,[23,27] may be explained by the fact that the magnetic orbitals are unfavorably oriented to interact. The good agreement between the fit and the experimental results seems to give substance to the dinuclear vision of the complex. However, the quite important intensity of the intermolecular interaction (zJ') could indicate the presence of a non-negligible second exchange pathway within the material. The 1-D model allows for a very nice fit of the experimental data, slightly better ($R^2 = 0.99991$ vs $R^2 = 0.99974$) than the one obtained with eq 1, with $g = 2.42$, $J_1 = -11.61$ cm^{-1}, and $J_2 = -3.02$ cm^{-1} (red lines in Figure 5). Nevertheless, strictly speaking, none of these models allow for the assignment of an exchange constant to a specific bridge. Therefore, we orientated our work toward EPR spectroscopy in solution and theoretical calculations to unambiguously elucidate the magnetic description of **4**.

EPR Spectroscopy. The idea of performing EPR measurements lies in the fact that in solution, the intermolecular hydrogen-bonding contacts are expected not to exist, while the intramolecular copper–copper interactions are still operating. Therefore, these measurements should unambiguously elucidate the possible occurrence of an exchange pathway through **4a**. The frozen methanol solution EPR spectrum for compound **4**, depicted in Figure 7, displays seven hyperfine lines in the parallel region, associated with the coupling of an electron with two nuclei with $S = 3/2$ such as either ^{63}Cu or ^{65}Cu. The forbidden transition $\Delta M_s = \pm 2$ is observed at $H = 1699$ G, thus confirming a ligand-mediated interaction between the Cu ions. Similar spectra have been described for dicopper(II) complexes with aliphatic spacers, with separation distances ranging from 6.9 to 9.1 Å.[91−94] For solutions of these complexes, as for the one discussed herein, the ligand σ bonds are the only possible channel of the spin–spin exchange interactions between the unpaired electrons in dinuclear copper(II) complex. This effect may be caused by a spin–spin polarization of the σ unit, or by the formation of extended molecular orbitals which include atoms of the spacer. Nevertheless, this experiment indicates unambiguously the occurrence of a magnetic exchange through **4a**.

Computational Studies. The magnetic properties have been further investigated by quantum chemical calculations, based on both DFT and wave function-based *ab initio* methodologies (see Computational Details). Calculations have been performed on two distinct dinuclear models (Figure 2), namely, **4a**, which illustrates a potential intramolecular Cu1···Cu1b interaction, and **4b**, which takes into account a possible Cu1···Cu1c interaction via nitrate/water hydrogen bonds. Such a strategy to consider a succession of dinuclear units (like in compound **4**) has already been used successfully in previous studies on magnetic chains.[95,96] This bottom-up-like approach should shed some light on the origin (i) of the antiferromagnetic behavior observed in **4** and (ii) of the relative participation of the different dinuclear subunits by the evaluation of J_a and J_b.

First, DFT calculations were performed on both dinuclear molecules. Even if debate on the proper use of the broken-symmetry approach for the calculation of magnetic coupling is still open (see Computational Details),[39−41] DFT has proved its potential for the calculation, with at least a qualitative accuracy, of exchange coupling constants in dinuclear copper

dx.doi.org/10.1021/ic200480d |*Inorg. Chem.* 2011, 50, 5696–5705

complexes.[97−100] To preclude any bias due to the use of a specific exchange-correlation functional, the calculations were carried out with either pure GGA (BP86), classical hybrid (B3LYP), or meta-GGA (M06) functionals (see Computational Details). As expected, the hybrid and meta-GGA functionals favor the triplet state in contrast to the BP86 functional (see Table 5). However, the results of all calculations suggest that the magnetic properties of **4** mostly arise from the intramolecular Cu1···Cu1b moiety, through the ligand dimp. With all functionals used, the J_b value is comparatively negligible for **4b** (Table 5). Thus, the conclusion drawn from the DFT calculations strongly differs from our first hypothesis, which assumes that the presence of sp^3 carbons into the dimp ligand may disrupt a potential intramolecular ligand-mediated exchange. One may suggest that this discrepancy may be attributed to a poor description of through-hydrogen-bond effects using such a DFT method without any *ad hoc* parametrization.

In order to clarify this particular issue, CAS[2,2] calculations (see Computational Details) were performed on the same dinuclear units (Figure 2). As expected, the magnetic orbitals are those of Cu d-type combinations with a small delocalization on the coordinated atoms of the square-pyramid base (Figure 8). In contrast with the DFT results, CAS[2,2]PT2 calculations (Table 5) suggest that both magnetic channels, i.e., through the dimp ligand (**4a**) and through H bonds (**4b**), may coexist with J_a still slightly higher than J_b. Finally, this important issue has been examined using DDCI calculations since the participation of hydrogen bonds can be explicitly included in this procedure by expanding the active space.[35] At the highest level of calculation with minimal active space, i.e., CAS[2,2]+DDCI-3, the calculated exchange-coupling constant is -2.8 cm^{-1} for **4a** and $+1.7$ cm^{-1} for **4b** (see Table 5). For both dinuclear molecules, the small interaction originates from the weak overlap between the magnetic orbitals coupled with a long Cu···Cu distance, which induces a very small kinetic exchange.[38] However, this canonical approach with a minimal active space is still not satisfactory since at this level, the calculated J_a and J_b do not allow one to correctly simulate the magnetic data. As shown previously,[35] a significant enlargement of the active space may be required to include all of the contributions arising from the charge fluctuations within the through-H bridges. Hence, a CAS[10,8] including the hydrogen-bond backbone was used for the singlet−triplet energy difference calculation for the model **4b**. This particular active space aims at including the σ and σ^* MOs localized on the O−H bond as well as the lone pair localized on the O atom featuring the O−H···O bond. Even if the use of this enlarged CAS[10,8] discards any calculations beyond CAS[10,8]+DDCI-1, it has been shown previously that the insertion of the bridge MOs in the active space allows one to (i) incorporate the relevant physical mechanisms and (ii) reach spectroscopic accuracy.[101] Indeed, in the CAS[2,2] approach, the kinetic exchange is explicitly introduced. At a DDCI-3 level, this contribution is not only revisited but the mechanisms involving the bridging ligand MOs are turned on.[102] However, some mechanisms involving simultaneous charge reorganization within the hydrogen bonds (i.e., involving σ and σ^* MOs and lone pairs localized on the O−H···O fragments) and ligand-to-metal charge transfer are still absent and might play a determinant role. Thus, the CAS[10,8] strategy allows one to evaluate some contributions to superexchange which are not accessible with the minimal CAS[2,2] approach. The CAS[10,8]+DDCI-1 result (Table 5) illustrates a strong enhancement of the antiferromagnetic contribution to the exchange coupling J_b in **4b**

Table 5. Calculated Exchange Coupling Constant (J, in cm^{-1}) in Dinuclear Models 4a and 4b Using Various DFT or CI Computational Strategies[a]

	4a	4b
DFT (BP86)	−13.7 (−27.4)[b]	−0.8 (−1.6)
DFT (B3LYP)	−4.2 (−8.4)	−0.1 (−0.2)
DFT (M06)	−5.0 (−10.0)	+0.4 (+0.8)
CAS[2,2]PT2	−7.2	−5.9
CAS[2,2]+DDCI-3	−2.8	+1.7
CAS[10,8]+DDCI-1		−10.4

[a] For comparison, the experimental fitting of the data leads to (i) J = -11.40 cm^{-1} and zJ' = -2.32 cm^{-1} (Bleaney-Bowers) or (ii) J_1 = -11.61 cm^{-1} and J_2 = -3.02 cm^{-1} (Hatfield). [b] Exchange coupling constants obtained with the SP expression are given in parentheses.

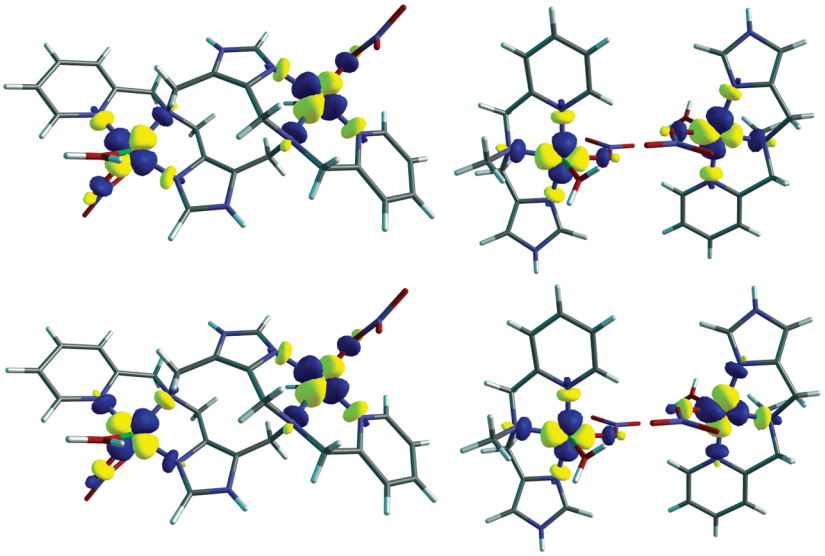

Figure 8. Magnetic molecular orbitals of **4a** (left) and **4b** (right).

dx.doi.org/10.1021/ic200480d |*Inorg. Chem.* 2011, 50, 5696–5705

(-10.4 vs $+1.7$ cm^{-1}). At this stage, the computed coupling constants for both dinuclear model systems ($J_a = -2.8$ cm^{-1} for **4a** and $J_b = -10.4$ cm^{-1} for **4b**) are in very good agreement with the experimental set of parameters (J_1, J_2) whatever the model used to describe the magnetic properties of **4**. More importantly, the leading interaction arises from the H-bonded dinuclear moieties, a rather nonintuitive picture for this material. Finally, this study emphasizes the necessity, for a reliable result, of adopting the computational strategy in order to properly take into account the specificities of the various magnetic coupling pathways.

CONCLUSIONS

A hydrogen-bonded 1D chain of dicopper(II) complexes has been obtained from a dinucleating ligand. This supramolecular polymer of dinuclear units is characterized by two different Cu···Cu separation distances within the chain, namely, 7.309(2) Å (intradinuclear) and 6.255(2) Å (interdinuclear). The shortest pathway is realized through very unusual hydrogen bonds involving a coordinated nitrate anion and water molecule. From the magnetic point of view, two models were tested to describe the magnetic properties: a dinuclear model with intermolecular interactions and 1-D chain with alternating interactions. Both approaches reveal the coexistence of two antiferromagnetic exchange pathways. However, from these measurements, the attribution of one exchange constant to a given exchange pathway is not possible. Solution EPR spectroscopy evidenced the presence of magnetic exchange through the dimp ligand, which cannot be ignored. Theoretical calculations based on both DFT and CI methodologies were conducted to clarify the magnetic measurements. Whereas DFT supports the magnetic coupling between the copper(II) ions mainly occurring via the longer intramolecular pathway, DDCI calculations ruled out this conclusion and predicted, as it was first anticipated based on the structural information, that the main magnetic channel corresponds to the intermolecular exchange interactions through hydrogen bonds. The anion/water bridge turns out to be a rather efficient magnetic channel probed by a specific active space enlargement which allows one to specifically turn on the H-bond contributions. On the basis of these findings, the magnetic properties may be interpreted considering **4** as an alternating antiferromagnetic 1D chain. This study nicely illustrates the importance of H-bond networks in the design of molecular architectures with potential magnetic properties. The role of such weak bonds is not only to structure materials but also to set up specific magnetic behavior. Finally, the interplay between experimental work and theoretical analysis was determined to conclude on this particular scenario. Following this strategy, an extended coupled experimental/theoretical study of the magnetic complexes of parent complexes is underway to get insights into the mechanisms behind the magnetic properties in such weakly interacting complexes.

ASSOCIATED CONTENT

Supporting Information. Figure S1 illustrating the crystal packing of **4**. This material is available free of charge via the Internet at http://pubs.acs.org.

AUTHOR INFORMATION

Corresponding Author

*E-mail: boris.le.guennic@ens-lyon.fr, patrick.gamez@qi.ub.es, gasquel@servidor.unam.mx.

ACKNOWLEDGMENT

P.G. acknowledges financial support from European Cooperation in the Field of Science and Technology (COST) Action D35/0011 and ICREA (Institució Catalana de Recerca i Estudis Avançats). B.L.G., V.R., and N.A.G.B. thank the ANR project "fdp magnets" for financial supports and the Pôle Scientifique de Modélisation Numérique (PSMN) at ENS de Lyon for computing facilities. J.S.C. acknowledges the Spanish Ministerio de Ciencia through the Juan de la Cierva Program number 18-08-463B-750.

REFERENCES

(1) Molenveld, P.; Engbersen, J. F. J.; Reinhoudt, D. N. *Chem. Soc. Rev.* **2000**, *29*, 75–86.
(2) Chin, J. *Acc. Chem. Res.* **1991**, *24*, 145–152.
(3) Solomon, E. I.; Tuczek, F.; Root, D. E.; Brown, C. A. *Chem. Rev.* **1994**, *94*, 827–856.
(4) Chufan, E. E.; Puiu, S. C.; Karlin, K. D. *Acc. Chem. Res.* **2007**, *40*, 563–572.
(5) Mirica, L. M.; Ottenwaelder, X.; Stack, T. D. P. *Chem. Rev.* **2004**, *104*, 1013–1045.
(6) Koval, I. A.; Gamez, P.; Belle, C.; Selmeczi, K.; Reedijk, J. *Chem. Soc. Rev.* **2006**, *35*, 814–840.
(7) Lewis, E. A.; Tolman, W. B. *Chem. Rev.* **2004**, *104*, 1047–1076.
(8) Allen, A. D.; Harris, R. O.; Loescher, B. R.; Stevens, J. R.; Whiteley, R. N. *Chem. Rev.* **1973**, *73*, 11–20.
(9) van Haaster, D. J.; Jongejan, J. A.; Hagedoorn, P. L.; Hagen, W. R. *Int. J. Hydrog. Energy* **2006**, *31*, 1432–1438.
(10) Bleaney, B.; Bowers, K. D. *Proc. R. Soc., London* **1952**, *A214*, 451–465.
(11) Mrozinski, J. *Coord. Chem. Rev.* **2005**, *249*, 2534–2548.
(12) Pardo, E.; Ruiz-Garcia, R.; Cano, J.; Ottenwaelder, X.; Lescouezec, R.; Journaux, Y.; Lloret, F.; Julve, M. *Dalton Trans.* **2008**, 2780–2805.
(13) Murray, K. S. *Eur. J. Inorg. Chem.* **2008**, 3101–3121.
(14) Ribas, J.; Escuer, A.; Monfort, M.; Vicente, R.; Cortes, R.; Lezama, L.; Rojo, T. *Coord. Chem. Rev.* **1999**, *193*−*5*, 1027–1068.
(15) Real, J. A.; Gaspar, A. B.; Niel, V.; Munoz, M. C. *Coord. Chem. Rev.* **2003**, *236*, 121–141.
(16) Thompson, L. K. *Coord. Chem. Rev.* **2002**, *233*, 193–206.
(17) Lozan, V.; Loose, C.; Kortus, J.; Kersting, B. *Coord. Chem. Rev.* **2009**, *253*, 2244–2260.
(18) Klingele, J.; Dechert, S.; Meyer, F. *Coord. Chem. Rev.* **2009**, *253*, 2698–2741.
(19) Ambrosi, G.; Formica, M.; Fusi, V.; Giorgi, L.; Micheloni, M. *Coord. Chem. Rev.* **2008**, *252*, 1121–1152.
(20) Klingele, M. H.; Brooker, S. *Coord. Chem. Rev.* **2003**, *241*, 119–132.
(21) Lehn, J.-M. *Supramolecular Chemistry: Concept and Perspective*; VCH: Weinheim, Germany, 1995.
(22) Luna-Ramirez, K. S.; Bernes, S.; Gasque, L. *Acta Crystallogr., Sect. E* **2008**, *64*, M1135–U347.
(23) Gasque, L.; Ugalde-Saldivar, V. M.; Membrillo, I.; Olguin, J.; Mijangos, E.; Bernes, S.; Gonzalez, I. *J. Inorg. Biochem.* **2008**, *102*, 1227–1235.
(24) Gasque, L.; Mijangos, E.; Ortiz-Frade, L. *Acta Crystallogr., Sect. E* **2005**, *61*, M673–M676.
(25) Driessen, W. L.; Rehorst, D.; Reedijk, J.; Mutikainen, P.; Turpeinen, U. *Inorg. Chim. Acta* **2005**, *358*, 2167–2173.
(26) Gasque, L.; Olguin, J.; Bernes, S. *Acta Crystallogr., Sect. E* **2005**, *61*, M274–M276.
(27) Mendoza-Diaz, G.; Driessen, W. L.; Reedijk, J.; Gorter, S.; Gasque, L.; Thompson, K. R. *Inorg. Chim. Acta* **2002**, *339*, 51–59.
(28) Gonzalez-Sebastian, L.; Ugalde-Saldivar, V. M.; Mijangos, E.; Mendoza-Quijano, M. R.; Ortiz-Frade, L.; Gasque, L. *J. Inorg. Biochem.* **2010**, *104*, 1112–1118.

(29) Moreno, J. M.; Ruiz, J.; Dominguez-Vera, J. M.; Colacio, E. *Inorg. Chim. Acta* **1993**, *208*, 111–115.
(30) Plass, W.; Pohlmann, A.; Rautengarten, J. *Angew. Chem., Int. Ed.* **2001**, *40*, 4207–4210.
(31) Valigura, D.; Moncol, J.; Korabik, M.; Pucekova, Z.; Lis, T.; Mrozinski, J.; Melnik, M. *Eur. J. Inorg. Chem.* **2006**, 3813–3817.
(32) Tang, J. K.; Costa, J. S.; Golobic, A.; Kozlevcar, B.; Robertazzi, A.; Vargiu, A. V.; Gamez, P.; Reedijk, J. *Inorg. Chem.* **2009**, *48*, 5473–5479.
(33) Vaskova, Z.; Moncol, J.; Korabik, M.; Valigura, D.; Svorec, J.; Lis, T.; Valko, M.; Melnik, M. *Polyhedron* **2010**, *29*, 154–163.
(34) Desplanches, C.; Ruiz, E.; Rodriguez-Fortea, A.; Alvarez, S. *J. Am. Chem. Soc.* **2002**, *124*, 5197–5205.
(35) Le Guennic, B.; Ben Amor, N.; Maynau, D.; Robert, V. *J. Chem. Theory Comput.* **2009**, *5*, 1506–1510.
(36) Sheldrick, G. M. University of Göttingen: Göttingen, Germany, 1997.
(37) Wilson, A. J. C. *International Tables for Crystallography*; Kluwer Academic Publishers: Dordrecht, The Netherlands, 1995; Vol. C.
(38) Kahn, O. *Molecular Magnetism*; Wiley-VCH: Weinheim, German, 1993.
(39) Velde, G. T.; Bickelhaupt, F. M.; Baerends, E. J.; Guerra, C. F.; Van Gisbergen, S. J. A.; Snijders, J. G.; Ziegler, T. *J. Comput. Chem.* **2001**, *22*, 931–967.
(40) Ruiz, E.; Cano, J.; Alvarez, S.; Alemany, P. *J. Comput. Chem.* **1999**, *20*, 1391–1400.
(41) Caballol, R.; Castell, O.; Illas, F.; Moreira, I.; de, P. R.; Malrieu, J. P. *J. Phys. Chem. A* **1997**, *101*, 7860–7866.
(42) Moreira, I.; de, P. R.; Illas, F. *Phys. Chem. Chem. Phys.* **2006**, *8*, 1645–1659.
(43) Ruiz, E.; Cano, J.; Alvarez, S.; Polo, V. *J. Chem. Phys.* **2006**, *124*, 107102.
(44) Adamo, C.; Barone, V.; Bencini, A.; Broer, R.; Filatov, M.; Harrison, N. M.; Illas, F.; Malrieu, J. P.; Moreira, I.; de, P. R. *J. Chem. Phys.* **2006**, *124*, 107101.
(45) Noodleman, L.; Norman, J. G. *J. Chem. Phys.* **1979**, *70*, 4903–4906.
(46) Noodleman, L. *J. Chem. Phys.* **1981**, *74*, 5737–5743.
(47) Ruiz, E.; Alemany, P.; Alvarez, S.; Cano, J. *J. Am. Chem. Soc.* **1997**, *119*, 1297–1303.
(48) Ruiz, E.; Alvarez, S.; Rodríguez-Fortea, A.; Alemany, P.; Pouillon, Y.; Massobrio, C. In *Magnetism: Molecules to Materials*; Miller, J. S., Drillon, M., Eds.; Wiley-VCH: Weinheim, German, 2001; Vol. 2, p 227.
(49) Ruiz, E.; Alvarez, S.; Cano, J.; Polo, V. *J. Chem. Phys.* **2005**, *123*, 164110.
(50) Desplanches, C.; Ruiz, E.; Rodriguez-Fortea, A.; Alvarez, S. *J. Am. Chem. Soc.* **2002**, *124*, 5197–5205.
(51) Schwabe, T.; Grimme, S. *J. Phys. Chem. Lett.* **2010**, *1*, 1201–1204.
(52) Peralta, J. E.; Melo, J. I. *J. Chem. Theory Comput.* **2010**, *6*, 1894–1899.
(53) Ruiz, E. *Chem. Phys. Lett.* **2008**, *460*, 336–338.
(54) Valero, R.; Costa, R.; Moreira, I.; de, P. R.; Truhlar, D. G.; Illas, F. *J. Chem. Phys.* **2008**, *128*, 114103.
(55) Becke, A. D. *Phys. Rev. A* **1988**, *38*, 3098–3100.
(56) Perdew, J. P. *Phys. Rev. B* **1986**, *33*, 8822–8824.
(57) Lee, C. T.; Yang, W. T.; Parr, R. G. *Phys. Rev. B* **1988**, *37*, 785–789.
(58) Becke, A. D. *J. Chem. Phys.* **1993**, *98*, 5648–5652.
(59) Vosko, S. H.; Wilk, L.; Nusair, M. *Can. J. Phys.* **1980**, *58*, 1200–1211.
(60) Zhao, Y.; Truhlar, D. G. *Theor. Chem. Acc.* **2008**, *120*, 215–241.
(61) Ruiz, E. *Chem. Phys. Lett.* **2008**, *460*, 336–338.
(62) Roos, B. O. *Adv. Chem. Phys.* **1987**, *69*, 399–445.
(63) Karlstrom, G.; Lindh, R.; Malmqvist, P. A.; Roos, B. O.; Ryde, U.; Veryazov, V.; Widmark, P. O.; Cossi, M.; Schimmelpfennig, B.; Neogrady, P.; Seijo, L. *Comput. Mater. Sci.* **2003**, *28*, 222–239.
(64) Miralles, J.; Daudey, J. P.; Caballol, R. *Chem. Phys. Lett.* **1992**, *198*, 555–562.
(65) Miralles, J.; Castell, O.; Caballol, R.; Malrieu, J. P. *Chem. Phys.* **1993**, *172*, 33–43.
(66) Ben Amor, N.; Maynau, D. *Chem. Phys. Lett.* **1998**, *286*, 211–220.
(67) Herebian, D.; Wieghardt, K. E.; Neese, F. *J. Am. Chem. Soc.* **2003**, *125*, 10997–11005.
(68) Messaoudi, S.; Robert, V.; Guihery, N.; Maynau, D. *Inorg. Chem.* **2006**, *45*, 3212–3216.
(69) de Graaf, C.; Illas, F. *Phys. Rev. B* **2001**, *63*, 13.
(70) Illas, F.; Moreira, I.; de, P. R.; de Graaf, C.; Barone, V. *Theor. Chem. Acc.* **2000**, *104*, 265–272.
(71) Le Guennic, B.; Petit, S.; Chastanet, G.; Pilet, G.; Luneau, D.; Ben Amor, N.; Robert, V. *Inorg. Chem.* **2008**, *47*, 572–577.
(72) Le Guennic, B.; Robert, V. *C. R. Chim.* **2008**, *11*, 650–664.
(73) Chastanet, G.; Le Guennic, B.; Aronica, C.; Pilet, G.; Luneau, D.; Bonnet, M. L.; Robert, V. *Inorg. Chim. Acta* **2008**, *361*, 3847–3855.
(74) de Graaf, C.; Sousa, C.; Moreira, I. D.; Illas, F. *J. Phys. Chem. A* **2001**, *105*, 11371–11378.
(75) Queralt, N.; Taratiel, D.; de Graaf, C.; Caballol, R.; Cimiraglia, R.; Angeli, C. *J. Comput. Chem.* **2008**, *29*, 994–1003.
(76) Andersson, K.; Malmqvist, P. A.; Roos, B. O.; Sadlej, A. J.; Wolinski, K. *J. Phys. Chem.* **1990**, *94*, 5483–5488.
(77) Andersson, K.; Malmqvist, P. A.; Roos, B. O. *J. Chem. Phys.* **1992**, *96*, 1218–1226.
(78) Roos, B. O.; Lindh, R.; Malmqvist, P. A.; Veryazov, V.; Widmark, P. O. *J. Phys. Chem. A* **2005**, *109*, 6575–6579.
(79) Roos, B. O.; Lindh, R.; Malmqvist, P. A.; Veryazov, V.; Widmark, P. O. *J. Phys. Chem. A* **2004**, *108*, 2851–2858.
(80) Widmark, P. O.; Malmqvist, P. A.; Roos, B. O. *Theor. Chim. Acta* **1990**, *77*, 291–306.
(81) Dewan, J. C.; Lippard, S. J. *Inorg. Chem.* **1980**, *19*, 2079–2082.
(82) Kolks, G.; Lippard, S. J. *Acta Crystallogr., Sect. C* **1984**, *40*, 261–271.
(83) Nicholson, G. A.; Petersen, J. L.; McCormick, B. J. *Inorg. Chem.* **1982**, *21*, 3274–3280.
(84) Addison, A. W.; Rao, T. N.; Reedijk, J.; van Rijn, J.; Verschoor, G. C. *J. Chem. Soc., Dalton Trans.* **1984**, 1349–1356.
(85) Burley, S. K.; Petsko, G. A. *Science* **1985**, *229*, 23–28.
(86) Gamez, P.; Mooibroek, T. J.; Teat, S. J.; Reedijk, J. *Acc. Chem. Res.* **2007**, *40*, 435–444.
(87) Mooibroek, T. J.; Black, C. A.; Gamez, P.; Reedijk, J. *Cryst. Growth Des.* **2008**, *8*, 1082–1093.
(88) Mooibroek, T. J.; Gamez, P.; Reedijk, J. *CrystEngComm* **2008**, *10*, 1501–1515.
(89) Schottel, B. L.; Chifotides, H. T.; Dunbar, K. R. *Chem. Soc. Rev.* **2008**, *37*, 68–83.
(90) Hall, J. W.; Marsh, W. E.; Weller, R. R.; Hatfield, W. E. *Inorg. Chem.* **1981**, *20*, 1033–1037.
(91) Monzani, E.; Quinti, L.; Perotti, A.; Casella, L.; Gullotti, M.; Randaccio, L.; Geremia, S.; Nardin, G.; Faleschini, P.; Tabbi, G. *Inorg. Chem.* **1998**, *37*, 553–562.
(92) Mandal, S. K.; Thompson, L. K.; Newlands, M. J.; Gabe, E. J.; Lee, F. L. *Inorg. Chem.* **1990**, *29*, 3556–3561.
(93) Tandon, S. S.; Thompson, L. K.; Bridson, J. N.; Dewan, J. C. *Inorg. Chem.* **1994**, *33*, 54–61.
(94) Larin, G. M.; Minin, V. V.; Shulgin, V. F. *Usp. Khimii* **2008**, *77*, 476–490.
(95) Pilet, G.; Medebielle, M.; Tommasino, J. B.; Chastanet, G.; Le Guennic, B.; Train, C. *Eur. J. Inorg. Chem.* **2009**, 4718–4726.
(96) Bonnet, M. L.; Aronica, C.; Chastanet, G.; Pilet, G.; Luneau, D.; Mathonière, C.; Clerac, R.; Robert, V. *Inorg. Chem.* **2008**, *47*, 1127–1133.
(97) Ruiz, E.; Alemany, P.; Alvarez, S.; Cano, J. *J. Am. Chem. Soc.* **1997**, *119*, 1297–1303.
(98) Ruiz, E.; Alvarez, S.; Rodríguez-Fortea, A.; Alemany, P.; Pouillon, Y.; Massobrio, C. In *Magnetism: Molecules to Materials*; Miller, J. S., Drillon, M., Eds.; Wiley-VCH: Weinheim, Germany, 2001; Vol. 2, p 227.

(99) Ruiz, E.; Alvarez, S.; Cano, J.; Polo, V. *J. Chem. Phys.* **2005**, *123*, 164110.
(100) Desplanches, C.; Ruiz, E.; Rodriguez-Fortea, A.; Alvarez, S. *J. Am. Chem. Soc.* **2002**, *124*, 5197–5205.
(101) Gellé, A.; Munzarova, M. L.; Lepetit, M. B.; Illas, F. *Phys. Rev. B* **2003**, *68*, 125103.
(102) de Loth, P.; Cassoux, P.; Daudey, J. P.; Malrieu, J. P. *J. Am. Chem. Soc.* **1981**, *103*, 4007–4016.